DTU Library

Modelling mitigation measures for smolt migration at dammed river sections

Azabo-Meszaros, Marcell; Forseth, Torbjørn; Baktoft, Henrik; Fjeldstad, Hans-Petter; Silva, Ana T.; Gjelland, Karl Øystein; Økland, Finn; Uglem, Ingebrigt; Alfredsen, knut

Published in:
Ecohydrology (Online)

Link to article, DOI:
10.1002/eco.2131

Publication date:
2019

Document Version
Publisher's PDF, also known as Version of record

Received: 11 October 2018 | Revised: 16 June 2019 | Accepted: 17 June 2019

DOI: 10.1002/eco.2131

RESEARCH ARTICLE

WILEY

Modelling mitigation measures for smolt migration at dammed river sections

Marcell Szabo-Meszaros[1] | Torbjørn Forseth[2] | Henrik Baktoft[3] | Hans-Petter Fjeldstad[4] | Ana T. Silva[2] | Karl Øystein Gjelland[5] | Finn Økland[2] | Ingebrigt Uglem[2] | Knut Alfredsen[1]

[1] Department of Civil and Environmental Engineering, Norwegian University of Science and Technology, Trondheim, Norway

[2] Norwegian Institute for Nature Research (NINA), Trondheim, Norway

[3] National Institute of Aquatic Resources, Technical University of Denmark, Silkeborg, Denmark

[4] SINTEF Energy Research, Trondheim, Norway

[5] Norwegian Institute for Nature Research (NINA), Tromsø, Norway

Correspondence

Marcell Szabo-Meszaros, Department of Civil and Environmental Engineering, Norwegian University of Science and Technology, S. P. Andersens 5, Trondheim 7491, Norway.
Email: marcell.szabo-meszaros@ntnu.no

Funding information

Norges Forskningsråd, Grant/Award Number: 244022

Abstract

There is no generic solution to establish safe passage of downstream-migrating fish passed hydropower facilities, and mitigation measures are species and site specific. Development of solutions is thus often based on "trial and error," and modelling-based approaches may significantly reduce cost and time to arrive at successful mitigation. Here, we explore such an approach by combining data on fish migration and hydraulic modelling. First, we performed a positional telemetry study at a dammed section of a Norwegian river, where 100 Atlantic salmon smolts were tagged to track their downstream movement at the vicinity of a hydropower intake channel and bypass gates. An explanatory model was developed to explore mechanisms of migration route, into the intake towards the turbines or through the bypass gates. Next, flow conditions during the smolt run was numerically modelled to explore the physical environment of the tracked smolts. The joint results from the two approaches supported the general assumption that downstream migration is strongly influenced by flow patterns and showed that fish entering the study site closer to the riverbank where the intake channel is located were more likely to enter the intake due to the strong currents towards the intake. Finally, a suite of measures to guide salmon smolts past the hydropower intake were proposed based on the findings and local conditions and tested by hydraulic modelling. We found that most of the measures that were likely candidates for field trials would most likely fail at improving safe passage, and only a rack-type guiding boom was promising. The presented combination of telemetry migration data and hydraulic modelling illustrates the value of evaluation of mitigation measures prior to implementation.

KEYWORDS

Atlantic salmon, downstream migration, ecohydraulics, hydraulic modelling, mitigation assessment

1 | INTRODUCTION

Hydropower plants (HPPs) on rivers are often detrimental to the fluvial fauna, and migratory fish species are particularly influenced by river fragmentations (Bunt, Castro-Santos, & Haro, 2012; Metcalfe & Craig, 2012). During their migration towards to the ocean, Atlantic salmon smolts (*Salmo salar* L.) may face flow diversion at water intake sites where route choice is crucial for successful downstream passage (Larinier, 2008). Different mitigation measures have been applied to guide the fish away from hydropower intakes (Albayrak, Kriewitz, Hager, & Boes, 2018; Boes, Albayrak, Kriewitz, & Peter, 2016; EPRI & DML, 2001) or attract them towards a bypass facility (Calles, Karlsson, Hebrand, & Comoglio, 2012; Scruton et al., 2007). A general solution does not exist, and mitigation measures are usually case specific and a function of local morphological, hydrological, operational, and ecological factors. Typically, extensive monitoring at each site is needed to identify the key criteria for successful mitigation (Wilkes et al., 2018), followed by monitoring of passage success of implemented measures (Silva et al., 2018). Downstream migration solutions thus often depend on a "trial and error" approach (Katopodis & Williams, 2012), sometimes followed by revisions of the measure. The "trial, error, and revision" approach is typically expensive and time consuming due to the necessary monitoring before and after implementation. To reduce time and cost, there is a need for better tools to test different measures without actual implementation.

Telemetry studies have provided valuable information on fish behaviour and migration route during downstream migration past HPP structures (Calles et al., 2010; Jansen, Winter, Bruijs, & Polman, 2007; Li et al., 2018; Nyqvist et al., 2017; Pedersen et al., 2012; Thorstad et al., 2017) and have been used to develop (e.g., Fjeldstad et al., 2012), evaluate, and adjust mitigation measures (e.g., Calles, Karlsson, Vezza, Comoglio, & Tielman, 2013; Havn et al., 2017; Scruton, McKinley, Kouwen, Eddy, & Booth, 2003). The combination of more detailed migration data from telemetry studies and numerical modelling of the flow field around artificial barriers could support the mitigation process significantly.

Computational fluid dynamics (CFD) in 3D has been used to explore relevant hydraulic conditions for target species in a fishway (Fuentes-Perez et al., 2018) and to assess the attraction flow at a hydropower plant (Gisen, Weichert, & Nestler, 2017). Moreover, Goodwin, Nestler, Anderson, Weber, and Loucks (2006) developed an algorithm that was able to forecast response of downstream migrating individuals and fish schools to specific hydraulic conditions in order to evaluate alternative bypass designs. Nestler, Goodwin, Smith, Anderson, and Li (2008) explored hydrodynamic cues used by outmigration juvenile salmon and concluded that their swimming path can explained by fluid dynamics and geomorphology and linked to sensory capacities of the fish. Khan, Roy, and Rashid (2008) utilized the same approach and demonstrated how CFD models could help to assess complex hydraulic engineering problems in relation with juvenile fish migration over dams. However, the potential for in situ combination of telemetry data with 3D hydraulic modelling to obtain successful downstream migration solutions is largely unexplored.

In the present study, we combine telemetry migration data and CFD to evaluate a suite of different methods to guide migrating Atlantic salmon smolt past a hydropower intake. For that, the telemetry data are used to explore migration patterns and route choice in relation to governing flow patterns as revealed by CFD. Next, we use these patterns to explore different mitigation measures in the CFD model and evaluate to what extent the measures are likely to guide fish past the hydropower intake. By doing so, we illustrate the value of using combined modelling to test mitigation measures prior to implementation and to reduce the need for the "trial, error, and revision" practice.

2 | MATERIALS AND METHODS

2.1 | Study site

This study was carried out at the Bjørset intake to the Svorkmo hydropower plant in the River Orkla in Central-Norway (63°03′18.7″N, 9°39′47.8″E). During parts of the smolt migration period, the majority of the flow goes towards the HPP intake, and high fish mortality is expected in the high-head HPP with Francis turbines. The intake is controlled by a dam with four identical gates (closed height and maximum operational water surface elevation: 129.50 m above sea level [m a.s.l.]; minimum water surface elevation throughout the field surveys: 129.10 m a.s.l.) and pool and weir-type fishways near each bank to allow passage of upstream migrating Atlantic salmon (Figure 1). Due to the low head (1.80 m), the fishways and gates represent safe passage opportunities for smolts. From May 1 to October 31, the northernmost gate (Gate 1) is open to release the stipulated minimum flow (20 $m^3\ s^{-1}$) whereas the other gates are used during flood conditions. For the remainder of the year, minimum flow (4 $m^3\ s^{-1}$ during winter) is released through the northern fishway. Approximately 100 m upstream from the dam an intake channel is located at the north side of the river. The intake area provide water through the intake channel and tunnel to the Svorkmo hydropower plant with a maximum capacity of 55 $m^3\ s^{-1}$. A concrete wall has been placed at the entrance of the intake channel with two openings at the bottom (1.5 × 25.8 m each) to prevent smolt (and ice or debris) to enter the intake channel. The top of the openings are 2.0–2.5 m below the water surface, depending on the river water level. Due to the relative small area of the openings in the wall (77.4 m^2) combined with the flow capacity, racks that prevents smolt entry (recommended 10- to 15-mm bar spacing; Fjeldstad, Pulg, & Forseth, 2018) cannot be installed in front of the wall without risk of impingement and mortality at the rack (DWA, 2005). This study was carried out in the dammed intake area, which is approximately 500 m long and 80–100 m wide with an average water depth of 2.5 m (Figure 1).

2.2 | Fish telemetry, positioning, and statistical analyses

During the smolt migration from late April to early June 2016, Atlantic salmon smolts were trapped 1,800 m upstream of the study site, and

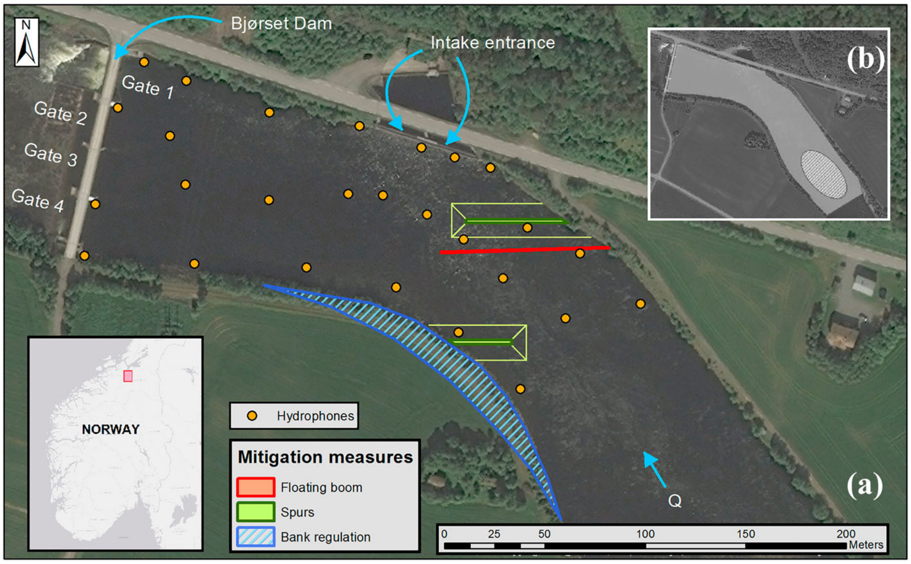

FIGURE 1 Study site at the Bjørset Dam at River Orkla in Central Norway with hydrophone positions and the location of three mitigation measures (Panel A). The modelled section and the deposited sediment (pattern shaded) at the upstream part are presented in Panel B. Background image source: ArcGIS® software by Esri (www.esri.com)

100 individuals were tagged with acoustic transmitters (Lotek, 200 kHz, model M-626, 7.5 × 17 mm, Lotek Wireless Inc., Newmarket, Ontario, Canada) with a 2.01 s burst interval. Fish were anaesthetized by immersion in an aqueous solution of 2-phenoxy-ethanol (0.7 ml l^{-1}, Sigma Chemical Co., St. Louis, MO, USA) and then placed ventral side up onto a V-shaped surgical table. An incision (~1 cm) was made with a scalpel on the ventral surface posterior to the pelvic girdle. The transmitter was inserted through the incision and pushed into the body cavity in front of the pelvic girdle. The incision was closed with two independent sutures (5/0, Ethicon, Prolene). During surgery, a 25 mg l^{-1} solution of 2-phenoxy-ethanol was circulated over the gills. Body mass (*M*), length (*L*), and smolt index (which indicates the parr–smolt transition of an individual, I_S, Johnston & Eales, 1970) were recorded as biotic parameters for all tagged fish (Table 1). After tagging, fish were left to recover from the surgery before being released.

Twenty-seven acoustic receivers (Lotek 200 kHz WHS 3050) were installed in the study site (Figure 1) and positioned using a GNSS receiver with a VRS-service providing 2 cm accuracy (CPOS-service from the Norwegian Mapping Authority). Receivers were either fixed on the concrete structures with the hydrophone at 70 cm depth or on a pole.

The detections of each smolt from the different hydrophones were processed by the software package YAPS (Baktoft, Gjelland, Økland, & Thygesen, 2017) to obtain movement trajectories including associated error estimates (standard deviation). This procedure produced migration tracks of each smolt with a position every 2 s. In total, migration tracks were obtained for 91 out of the 100 tagged smolts. Among the remaining nine smolts, one provided invalid data (apparently suffered predation), and eight smolts never appeared at the study site. Estimated positions with high uncertainty (i.e., *SD* > 5.0 m) were excluded from further analyses.

Timing of the last observation of each smolt was paired with the hourly observed abiotic parameters, such as water level (W_{elev}, m a.s.l.), total inflow (Q_{in}, $m^3\ s^{-1}$), flow through the dam (Q_{dam}, $m^3\ s^{-1}$), flow in the HPP intake (Q_{intake}, $m^3\ s^{-1}$), and the number of gates open (Nr_{Gates}) at the dam. Smolt generally passed rapidly through the area, and flow conditions at the last observation is a good representation of the hydrological conditions. The last position also determined the migration route (intake or one of the gates).

Watson's two-sample test (Mardia & Jupp, 2010) was used to test differences between the smolts migrating into the intake and through the gates (Smolt Groups A and B, Table 1). The smolt migration route was analysed using generalized linear models. A binomial model with logit-link function (Zuur, Hilbe, & Ieno, 2013) was used to derive a relationship between migration route (0 = gates, 1 = intake) and different environmental variables. The aforementioned W_{elev}, Q_{in}, Q_{intake}, and Nr_{Gates} variables and the ratio of the flow through the dam and intake channel (Q_{dam}/Q_{intake}) were added as hydrological and

TABLE 1 The average (±*SD*) body mass (*M*), length (*L*), smolt index (I_S) and Fulton's condition factor (*K*) for the 91 smolts included in the study, sorted according to their migration route (dam or hydropower plant intake)

Groups	Route	*n*	*M* (g)	*L* (cm)	I_S	*K*
A	Dam	74	22.45 ± 4.52	14.13 ± 0.91	2.3 ± 0.4	0.79 ± 0.08
B	Intake	17	21.12 ± 3.41	14.05 ± 0.79	2.3 ± 0.4	0.76 ± 0.09
Total		91	22.2 ± 4.35	14.12 ± 0.89	2.3 ± 0.4	0.78 ± 0.08

operational parameters to the model. In addition, time of the day (T_d, dusk-night-dawn or day), transversal distance to the south bank of the first registration of a smolt (D_S, m), and the residual of the log–log regression of smolt body mass (*M*, g) and length (*L*, cm) were entered as further explanatory variables. The Nr_{Gates} and T_d parameters were entered as categorical ones, whereas the others as continuous parameters. The statistical tests were performed using the R software (R Development Core Team, 2018) (used package: chron).

2.3 | Data for computational fluid dynamics modelling

Bathymetry data was collected using a SonTek M9 (San Diego, California) Acoustic Doppler Current Profiler (ADCP) from a boat across the modelled river reach (Figure 1, Panel B). The water elevation difference was controlled by a RTK-GPS (Leica Viva CS15) and found to be within the vertical accuracy of the instrument. Water velocities were measured in a transect at the upstream side of the dam while two of its gates were open during a flood event, by using the SonTek M9 ADCP for calibration purposes. In addition, four other transects were surveyed at the intake area by the same instrument to collect data to validate the model under different flow conditions. Each transect was measured six to eight times following the recommendation of Le Coz et al. (2016). The ADCP data were further processed by the Velocity Mapping Toolbox (v4.08; Parsons et al., 2013) for model calibration and validation. Geometry of the gates and the intake structure were taken from technical drawings and field measurements. The digitalized structures and bathymetry were combined into a geometry model. Discharge ranges in the river and through the dam and towards the HPP during the fish telemetry study are presented in Table 2.

2.4 | CFD modelling

Flow properties at the computational domain were captured by using one-phase *pimpleFoam* solver from OpenFOAM (Version 4.1.0, Greenshields, 2015), which discretise Reynolds-averaged Navier–Stokes equations and was associated with the standard k-ε turbulence model. The finite volume method to solve the equations by using the PIMPLE algorithm (Higuera, Lara, & Losada, 2013) for the pressure–velocity coupling and can compute the full 3D transient flow at the river site. The time step was adjusted dynamically according to the Courant–Friedrichs–Lewy condition at the value of 1.0, and it ranged between 3 and 9 ms in the different simulations. Each simulation was run on a high-performance computer distributed between 512 cores (simulation [wall] time: 4–7 days; computational cost: 25,000–50,000 hr per scenario).

The modelled river section was extended 200 m upstream of the telemetry area to allow properly development of the flow conditions at the telemetry site. Twelve comparable hexahedron-dominant computational mesh (two for the current condition and 10 for the mitigation measures; see Section 3.5 for details) were created by the *snappyHexMesh* utility of OpenFOAM.

The base computational grid (edge lengths: 0.35–0.60 m horizontally and 0.20 m vertically) had increased mesh resolution (edge lengths: 0.09–0.15 m horizontally and 0.05 m vertically) where details were necessary for assessment of fish migration. In addition, further refinement was made for the mesh around the implemented modifications at the mitigated cases, such as around spurs and floating guidance booms (see Section 3.5). The booms were modelled as either permeable or impermeable virtual barriers floating on the surface of the domain. The model of the permeable boom was based on one of the fish-friendly trash-rack design described by Szabo-Meszaros et al. (2018). In order to avoid the high number of cells at the immediate vicinity of the permeable boom with horizontal bars, the original design with 8 mm bar width and 15 mm bar gap was modified to reduce computational time. The rectangular bar elements and associated gaps were aggregated by merging every four elements, yielding 32-mm bar width and 60-mm bar gap configuration for the simulated case. The mesh size at each scenario consisted of 18 million cells.

As the majority of the tagged smolts moved through the study area when only one gate was open, such condition was modelled for low discharge (LQ) and high discharge (HQ) using OpenFOAM (see Table 2 for hydraulic boundary conditions). Simulated water velocity magnitudes (also known as resultant velocity, U_{mag} [m s^{-1}]) at 0.5 m below water surface were used to characterize the flow environment where the smolts were expected to travel (Thorstad, Whoriskey, Rikardsen, & Aarestrup, 2011).

After calibration, the two actual cases and 10 additional scenarios were prepared and simulated according to the desired mitigation conditions with the added elements. Simulated times were determined based on the flow development at the study site. The scenarios were set to represent 33 and 27 min of flow by simulation LQ and HQ conditions, respectively. Velocity field by CFD were used for further evaluation of the different mitigated conditions.

At the cases representing the LQ and HQ conditions, the release of five particles were modelled 0.5 m below water surface per section

TABLE 2 Summary of the operational (water elevation, W_{elev} [m a.s.l.]; number of gates open at the dam, Nr_{Gates} [–]) and discharge conditions (inlet, Q_{in} [m^3 s^{-1}]; through the dam, Q_{dam} [m^3 s^{-1}]; towards the HPP, Q_{intake} [m^3 s^{-1}]) at the domain during the telemetry survey in May 2016 (*Field*) and the chosen scenarios for simulation (CFD_{Low} and CFD_{High}). Q_{dam}/Q_{intake} is the dimensionless ratio between the two outlets

	W_{elev} (m a.s.l.)	Q_{in} (m^3 s^{-1})	Q_{dam} (m^3 s^{-1})	Q_{intake} (m^3 s^{-1})	Q_{dam}/Q_{intake}	Nr_{Gates}
Field	129.12–129.50	40.8–211.2	20.8–175.8	19.0–46.8	0.47–5.43	1–3
CFD_{Low}	129.12	51.9	22.0	29.9	0.73	1
CFD_{High}	129.44	112.1	66.6	45.5	1.46	1

at the upstream end of the study side with even distribution from the southern riverbank in four sections (south, central-south, central-north, and north). The *streamlines* postprocessing utility of OpenFOAM sample particles (with user-defined releasing location) were transported by the velocity field to generate streamlines. The simulated particle tracks represent the movement of individual virtual units in the domain with two outlet options (either left the domain through the dam or through the intake).

3 | RESULTS

3.1 | Calibration and validation of the model

The CFD model was calibrated by adjusting roughness to yield high correlation between modelled and measured cross-sectional velocities at the calibration transect (at a flow of 129 m^3 s^{-1}). The final Pearson's correlation (R^2) between the CFD and ADCP values was .74. Next, the model performance was validated against another four field measured cross-sectional velocities under different conditions (198 m^3 s^{-1}). The correlation between the ADCP and CFD values were 0.39, 0.61, 0.73, and 0.74 for the four sections. Deviating values occurred at the edge of the cross sections, close to the riverbanks. The one section with poor correlation (R^2: .39) was measured immediately upstream of the intake entrance, and the low correlation was most likely due to the strong turbulent flows at that sections. The remaining sections provided acceptable correlation considering that the validation included 2,400 individual velocity values with associated simulated data in three dimensions in total.

3.2 | Hydraulics

Both at the LQ and HQ, horizontal velocities (x and y directions) dominated the modelled area (Figure 2a,b), except at the immediate proximity of the intake entrance where strong downward velocity occurred due to the openings at the bottom (Figure 2c,d).

The maximum velocity magnitude (U_{mag}) was approximately 0.64 m s^{-1} at LQ and 1.0 m s^{-1} during HQ and appeared at the vicinity of the intake. Sediment deposition at the upstream part of the modelled area and outside of the telemetry study area has significant impact on the velocity field as it yielded a split streamflow with high velocities appearing along both riverbanks (Figure 2a,b). The U_{mag} along the north riverbank exceeded 0.6 m s^{-1} even at LQ, whereas it peaked at 0.52 m s^{-1} (at LQ) along the south riverbank. The streamflow along the north riverbank move into the intake at both LQ and HQ conditions whereas the streamflow at the south riverbank dominated the flow field towards the open dam gate, particularly at HQ. The flow field remained divided as it approached the intake and the dam. The flow diversion was more apparent at LQ through the entire study site. The streamflow between the intake and the dam was bounded by an extensive recirculation zone in association with dead-water zones (U_{mag} < 0.05 m s^{-1}) along the southern bank, present at both LQ and HQ, as long as only one gate was open. Overall, the relative distribution of velocities was similar under the HQ and LQ scenarios.

3.3 | Telemetry and passage success

A total of 91 smolts were detected at the study site during the period of May 5 to 21, of which 17 (19%) left the area through the

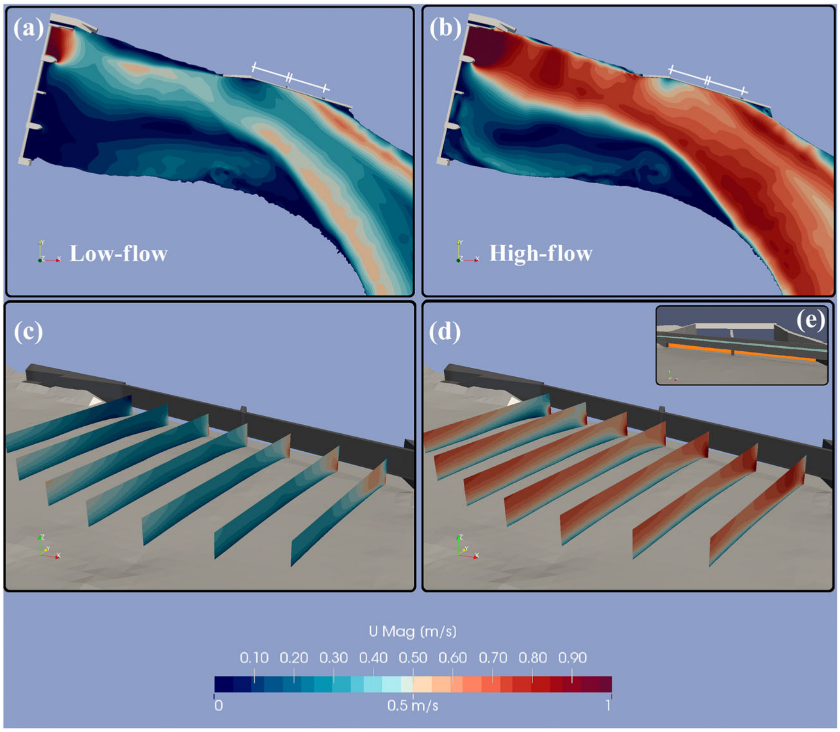

FIGURE 2 Simulated flow velocities at Bjørset Dam at 0.5 m below the water surface and at the intake entrance for LQ (a and c) and HQ conditions (b and d), respectively. The two openings at the intake are highlighted close to the river bed at Panel E. Note, lower velocity range was applied to the domain as the absolute highest velocity values (~2.0 m s^{-1}) only appeared at the gate outlets

hydropower intake (Table 1, Group A) and 74 (81%) smolts migrated past the dam gates (Table 1, Group B). Overall, 47 fish out of the detected 91 (52%) passed the domain while one gate was operated only at the dam. Thirteen individuals (28%) out of the 47 went into the intake during one gate operation, when the flow ranged between 22 and 66.6 $m^3\ s^{-1}$ and between 30 and 45.5 $m^3\ s^{-1}$ towards to the spillway (Q_{dam}) and to the intake channel (Q_{intake}), respectively. Out of the 13 fishes with passage to the HPP during one gate operation at the dam, five entered the intake at LQ, two at HQ, and the remaining at intermediate conditions. The remaining four fish out of the 17, which entered the intake, migrated during flood events when two or three gates were operated at the dam.

There was no significant difference between the groups, A and B, in terms of their passage time (Watson's two-sample test, $p > .05$). The median time of passage was 8 and 7 min for the Groups A and B, respectively. Smolts that passed through the dam swam on average 377 m in the study site, whereas individuals that entered the HPP intake swam 274 m on average. Overall, this information indicates that the majority of the smolts had active movement through the ~300-m study site without turning back or swimming upstream (Figure 3).

3.4 | The migration route model

Migration route modelling were performed with all (both biotic and abiotic) explanatory variables: $\text{logit}(\pi) = \log_{10}[\pi(1-\pi)^{-1}] = intercept + \beta_1 V_1 + \beta_2 V_2 + \ldots + \beta_8 V_8$, where π is the probability that fish leaves the domain through the intake, $\beta_1, \beta_2 \ldots \beta_8$ are the estimated coefficients, and $V_1, V_2 \ldots V_8$ are the different variables listed in Section 2.2. Variables in the full model were sequentially removed using the AIC (Akaike, 1974) value and by eliminating all variables that contribution was minor. The final model contained three variables: the discharge through intake (Q_{intake}), the number of open gates at the dam (Nr_{Gates}), and the distance of the starting position from the south bank (D_S) of each smolts as $\text{logit}(\pi) = \log_{10}[\pi(1-\pi)^{-1}] = \beta_1 Q_{intake} + \beta_2 Nr_{Gates} + \beta_3 D_S$ (Table 3).

According to the model a smolt is more likely to end up in the intake channel when the intake discharge (Q_{intake}) is high and if the smolt appear at the intake area close to the northern bank (high distance values, D_S). In contrast, the probability for intake passage is reduced if more gates are operated at the dam. (Nr_{gates}). Both, the Q_{intake} and Nr_{Gates} variables are influenced by the operation at the

TABLE 3 Estimated coefficient of the final migration route model with the three retained variables: Intake discharge (Q_{intake}), number of open gates at the dam (Nr_{Gates}), and the distance to the south bank at the first observance of a smolt (D_S)

Variable	Coefficient	Estimate	*SE*	*Z*	*p*
	Intercept	13.994	3.723	−3.759	<.001
Q_{intake}	ß$_1$	0.156	0.060	2.581	<.01
Nr_{Gates}: one	ß$_2$	2.099	0.905	2.320	<.05
D_S	ß$_3$	0.103	0.025	4.113	<.001

Svorkmo HPP, whereas the differences in arrival position can be due to upstream flow patterns feeding into the area and more random migration route selection.

To further illustrate the importance of the initial location for the final migration route selection, the first position of the smolts were sorted into four equally large sections across the river. Smolts that appeared close to the south bank (south and central-south sections) have much lower probability of intake passage than those which entered at the northern side of the river, closest to the intake (Figure 4). These sections corresponded to the governing hydraulic patterns at the entrance of the study area (northern section, high velocities towards to the HPP; central-north section, low velocities; and central-south and south sections, high velocities towards to the dam). Indeed, modelling five particle tracks at each sections at both flow conditions, produced a pattern where no particle entered the intake at the south section (one uncertain), followed by 10% (one uncertain; one particle at LQ), 70% (five particles at LQ and two at HQ), and 100% of the particles entering the intake in the sections towards the north.

3.5 | Mitigation measures

The two simulated scenarios revealed complex flow patterns at the entire study site, particularly at the proximity of the intake entrance (Figure 2). Streamflow along the north riverbank flows straight towards to the intake. It is generally assumed that downstream migrating salmon smolts follow the main flow (Rivinoja, 2005; Williams, Armstrong, Katopodis, Lariniere, & Travade, 2012), and the pattern observed and migration modelling in the present study strongly support this as a general migration pattern (Figure 4). We tested different mitigation measures that could either change the dominating flow

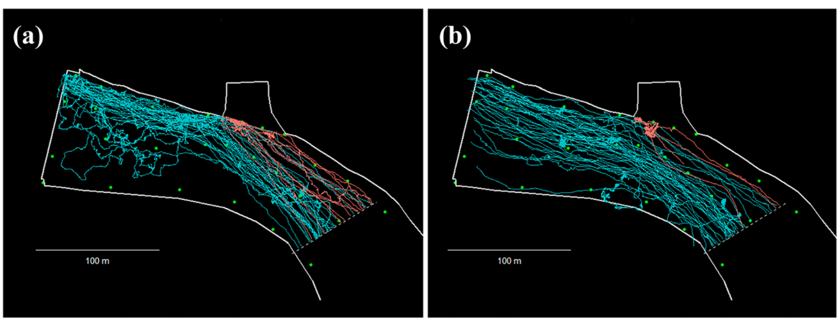

FIGURE 3 Fish tracks at the telemetry study site distributed according to gate operations (one gate open at Panel A and two or three gate open on Panel B. The different colours indicate the final destination of fish at the study site (blue, dam; red, intake)

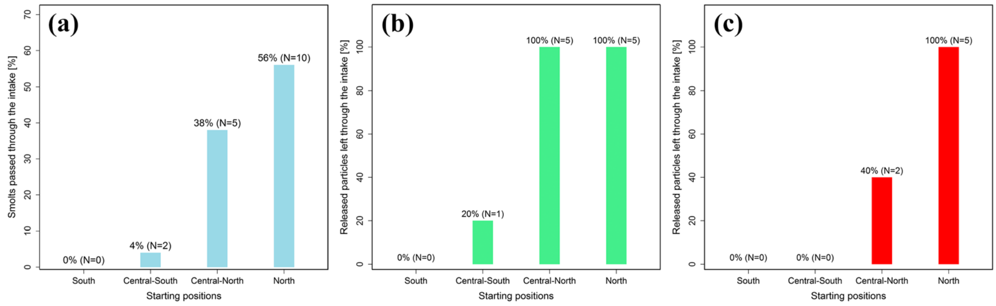

FIGURE 4 (a) The proportion of smolts with intake passage in relation to the distance of their first recorded position to the south bank, (b) the proportion of released particles (five particles per sections) with intake passage at LQ, and at (c) HQ as sorted into 20-m-wide sections (south, central-south, and etc)

patterns or guide the fish from the northern to the southern sections where stream flows towards the gates. The following mitigation measures were chosen as feasible options to test on the study site at the River Orkla:

1. Alternative gate usage at the Bjørset Dam, changing the open gate from the northernmost (Gate 1) to the southernmost (Gate 4).
2. Construction of spurs, also known as flow deflectors, groynes, dikes, or vanes, located at the vicinity of the intake channel, one at each riverbank. They had trapezoid cross section with 1:1 slope at the sides and 2-m-wide crest elevated at 129.50 m a.s.l., which is 0.0–0.5 m above water surface depending on the flow conditions. The length of their centreline was 30 m at the south riverbank, pointing upstream with a 28° angle and 40 m at the north river bank, pointing downstream with a 34° angle to the riverbank (location presented on Figure 1).
3. Modifying the curvature of the river section to increase the radius of the river bend and thereby influence the flow pattern. This was done by expanding the width of the river section by 20–25% (regulated bank section is presented in Figure 1).
4. Installation of floating fish guidance booms with 1.0 m submergence below the water surface (water depth under the boom ranged between 0.6–1.4 m) located at the upstream side of the intake channel at the north riverbank pointing downstream with an angle of 30°, following the findings of EPRI and DML (2001; location presented in Figure 1). The booms were modelled as a solid type (impermeable, 0.5m thickness) and as a trash-rack type (permeable, 0.064-m thickness). Both booms had a length of 75 m. The trash-rack type had horizontal bars, based on the fish-friendly trash-rack design described by Szabo-Meszaros et al. (2018). Some modifications of the rack were done to reduce computational cost (see Section 2.4).

On the basis of these four major mitigation types, 10 different mitigation cases (different combination of measures at two flow conditions, see Table 4) were simulated to evaluate their impact on the flow field and potential impact on smolt migration route. The latter was based on qualitative assessment of the flow fields and their directions (towards the intake or dam).

TABLE 4 Summary of the mitigation cases at the Bjørset Dam in the River Orkla tested with computational fluid dynamics modelling given by their ID, the type of measure, and flow condition

Mitigation ID	Mitigation measure	Flow condition
1.1	Alternative gate (AG)	Low
1.2	AG	High
2.1	Spurs, one at each river banks	Low
2.2	Spurs, one at each river banks + AG	Low
3.1	South bank regulation (width expansion)	Low
3.2	South bank regulation (width expansion) + AG	Low
4.1	Solid type floating boom (north bank)	Low
4.2	Solid type floating boom (north bank) + AG	Low
4.3	Rack type floating boom (north bank)	Low
4.4	Solid type floating boom (north bank) + AG	High

The first mitigation measures (1.1 and 1.2) simply involved changing the gate operation with the aim of shifting the main current closer to the southern bank, away from the intake area. It had only a marginal effect on the flow field in front of the intake (Figure 5a,b in comparison with Figure 2) but a large effect on the flow between the intake and the dam. Here, the main current was widened, the recirculation area at the south side was reduced, and a new recirculation area was formed at the upstream side of Gate 1. Due to the continued strong currents against the intake, this mitigation is unlikely to improve passage efficiency.

The second mitigation measure (2.1) was more extensive, involving the construction of spurs on both riverbanks at the upstream side of the intake, with the aim to change the flow pattern away from the intake area. This solution was also combined with alternative gate operation (2.2). The main effect was the joining of the two high velocity flows at the two banks into one major flow towards the lower part of the intake (Figure 5c,d). Velocities exceeding 1.0 m s^{-1} were seen at the new structures, but they abated as the current deflected towards the intake. Even higher velocities appeared locally at the downstream end of the intake, which dampened towards the dam. Changing the gate operation had no effect on the flow towards the intake, and

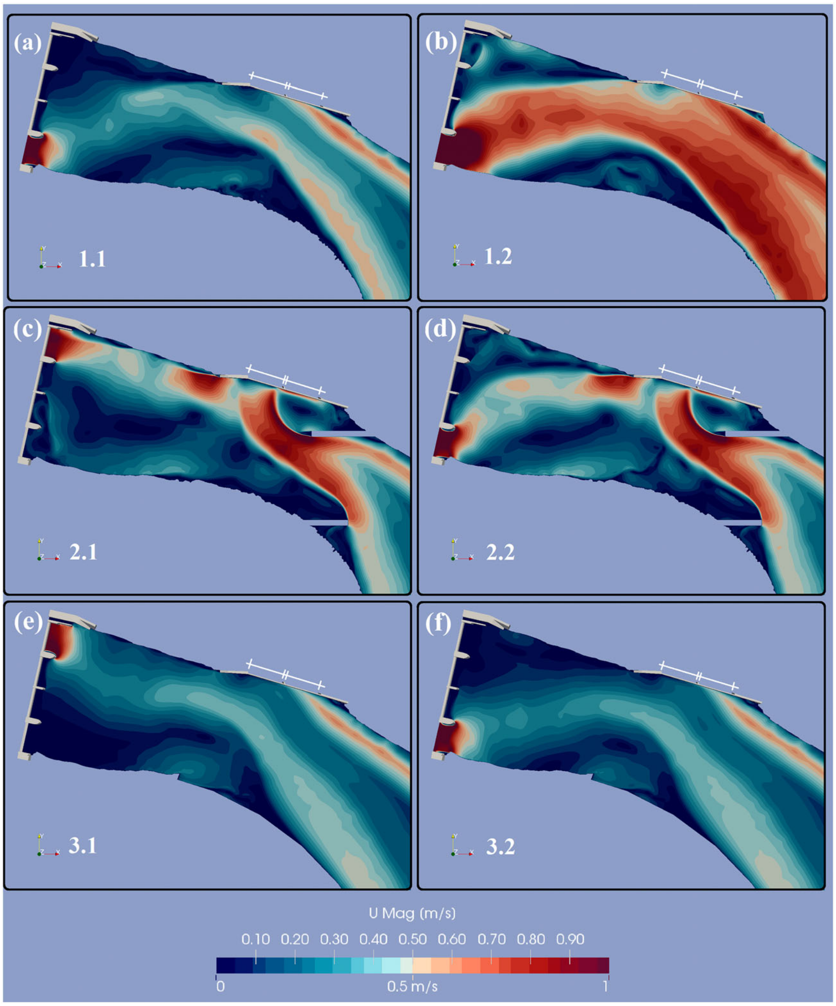

FIGURE 5 The effect of six mitigation cases (1.1–3.2) on the flow field at the Bjørset Dam. The impact of alternative gate operation (Gate 4) are presented for (a) LQ and (b) HQ, (c) effects of spurs are given for LQ with Gate 1 or (d) Gate 4 open, and (e) effects of expanding the river width with Gate 1 or (f) Gate 4 open. All velocity fields are from 0.5 m below the water surface. Note that lower velocity range was applied to the domain as the absolute highest velocity values (~2.0 m s^{-1}) only appeared at the gate outlets

the flow direction changed towards the south one-third downstream of the intake area. It is assumed that such a measure would have negative effects on smolt migration. Smolt that follows the southern streamflow that in the current conditions had a high probability of dam passage will most likely migrate with the new joint flow into the intake.

The third major measure (3.1) involved riverbank regulation on the south bank with the aim to reduce velocities and the main flows towards the intake. The width of the river at the bend was increased by approximately 20% to provide a larger area and potentially a more even flow field at the intake site. Here also, alternative gate operation was included (3.2). The streamflow along the south riverbank did indeed become wider (Figure 5e,f with reduced velocities ~0.40 m s^{-1} at 3.1 and 3.2 compared with ~0.50 m s^{-1} at the original LQ case in Figure 2), whereas the effect on the streamflow at the northern side was marginal. Therefore, the velocities overall decreased, although the velocity pattern remained similar to the original case, as the streamflow at the north side retained higher velocities compared with the streamflow at the south side. The effects on migration route are uncertain. If the across river distribution of smolts remain the same after bank regulation, the proportion of smolt entering the central and southern sections may be less likely to enter the intake. However, reduced velocities towards the southern bank may direct more smolts towards the high-risk northern flow.

Floating fish guidance booms were the fourth major mitigation types tested (4.1–4.4). Rather than directing the flow, the aim was to guide smolts from the northern to the southern bank. However, both solid and permeable floating booms were expected to influence flow fields, and this effect was explored (Figures 6 and 7). The guidance booms were modelled as a 1.0-m submerged solid or permeable (rack type) wall (Figure 7, Panels B and D, respectively). Both booms produced a more distinct southern flow pattern towards the open gate (Figure 6) than the current situation (Figure 2). The streamflow at the northern bank was dampened and its velocities decreased in all three simulations at LQ (4.1–4.3), because the boom divert the flow towards the south bank at the top of the water column. This effect was small for the permeable boom at LQ (Figure 6, Case 4.3, Panel C). In this case, the velocity patterns showed a more gradual distribution along the intake entrance compared with original case. The conditions at the mitigation case 4.3 is similar to the LQ simulation (Figure 6, Panel C compared with Figure 2, Panel A). When the fourth gate was opened, the solid boom provided a wide and continuous southern flow

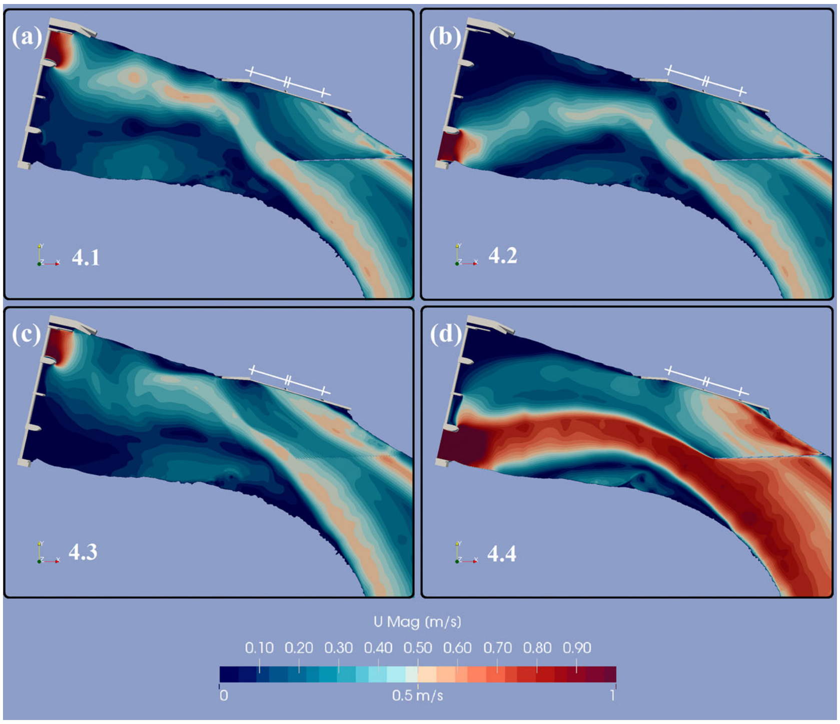

FIGURE 6 The effect of (a) solid and (c) permeable floating booms on the flow field at the Bjørset Dam under LQ conditions. The impact of solid type boom with alternative gate operation is presented at LQ (B) and at HQ (D). Note that lower velocity range was applied to the domain as the absolute highest velocity values (~2.0 m s^{-1}) only appeared at the gate outlets

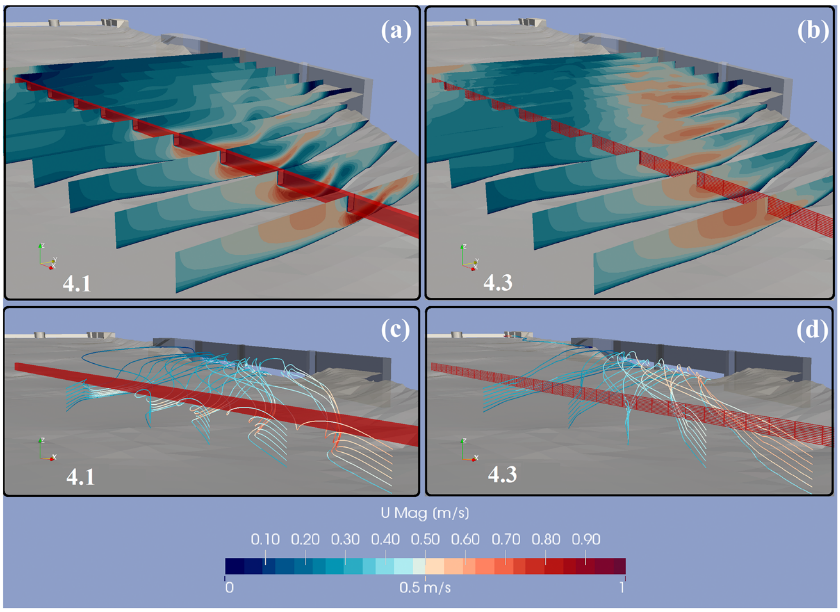

FIGURE 7 Velocity distribution in depth at the surroundings of the (a and b) solid and the (c and d) permeable floating booms. The upper panels (A and B) show the flow fields in vertical sections whereas the lower panels (C and D) show particle movement released at different depths upstream side of the booms. The plots were taken from the central section of the river looking downstream towards to the intake entrance (presented shaded grey model in the background)

towards the dam at HQ (Figure 6, Case 4.4, Panel D). Furthermore, at areas adjacent to the intake entrance and the boom, higher velocities were concentrated closer to the north riverbank. These features were not as prominent in the LQ cases (Figure 6a-c).

The booms strongly affected the velocity distribution in depth (Figure 7) at their immediate vicinity. The solid boom blocked the incoming flow at the top of the water column deflecting it under the device where, due to the local contraction, high velocities occur. The highest velocities remained downstream of the boom and emerge at the water surface as a vertical flow. Similar flow patterns appear under HQ condition (Case 4.4). In contrast, the permeable boom (a floating rack) had marginal downward velocities because the streamflow along the north river bank flows through the device.

The simulation of flow fields using solid and permeable floating booms provides information regarding their potential effects on smolt migration route. Although the solid boom had strong effects on the flow patterns in the study area, and particularly so at HQ, their guiding efficiency may be questioned because of the strong vertical downwards velocities at the upstream vicinity of the boom. The smolts may follow this flow and pass beneath the boom (Enders, Gessel, Anderson, & Williams, 2012). Indeed, the concrete wall extending from the surface and 2–2.5 m down in front of the HPP intake have vertical flows in the same magnitude and smolt appear to follow this flow into the intake channel (see Figure 2). Another potential challenge is the forces acting upon the boom during, for example, flood events, and to what extent such a boom could actually maintain its position. In conclusion, a solid boom would have low probability of guiding the fish towards the southern flow and through the gates and cannot be successfully used under the relevant flow conditions.

In contrast, the floating permeable boom may be more promising as a tool to influence migration route, because the northern flow pass through the boom and only moderate vertical downwards velocities were created. Because the fish cannot pass through the gaps, they might be guided along the boom and reach the southern flow area where the probability of gate passage is much higher. There are operational challenges with such a boom as well, for example, maintaining position and clean bars, which should be considered prior to implementation.

4 | DISCUSSION

In this paper, we combined general knowledge on Atlantic salmon smolt migration, local telemetry migration data, and migration route modelling with river section scale hydraulic modelling by CFD. The aim was to evaluate a suite of mitigation measures to prevent smolts from entering a hydropower intake and their migration through the turbines. Our primary aim was not to provide a solution for the particular case but rather to illustrate the value of combining knowledge on migration patterns with river reach hydraulic modelling as a novel tool to reduce the need for "trial and error" in designing downstream migration solutions in general.

The general assumption that downstream migrating salmon smolts follow the main flow (Rivinoja, 2005; Williams et al., 2012) was supported with several findings from the telemetry study. First, migration tracks showed that the smolts tended to enter and follow the two main streamflows along the two riverbanks, whereas the recirculation and dead-water zones were barely visited. Second, the developed migration route model showed that the route (intake or gates) was strongly dependent on the position of entry for the smolts to the study site. In agreement with simulated particle movement in the model, fish arriving closer to the southern riverbank were more likely to leave through the gates compared with smolts entering at the opposite bank where the intake is located. The southern flow goes towards the gates, whereas the northern flow goes into the intake. Third, the migration route model showed that high turbine flow and only one gate open at the dam increased the likelihood of smolts entering the intake. Higher flow through the HPP intake expand the width of the diverted flow towards to the HPP, whereas the number of operated gates counters it. A similar migration route model developed for a similar HPP intake location in southern Norway (Fjeldstad et al., 2012) showed that increased discharge into the intake increased the likelihood of salmon smolt turbine passage. More detailed analyses of links between the migration tracks and hydraulic properties at the study site are under development. However, for the present study, we used the simple "go with the main flow" and hydraulic modelling to evaluate the different mitigation measures.

The mitigation measures explored were based on altering flow patterns to move the main current away from the north bank and the HPP intake area and towards the south bank or to use guidance structures to move the smolt away from the northern bank and into southern flow against the gates in the dam.

None of the attempts to alter the flow by physical measures were very promising in terms of their likelihood of increasing dam passage. For instance, the spur design tested joint the northern and southern high velocity flows into one flow towards the intake, likely to increasing the proportion of smolts entering the HPP intake. Also, the high velocities in association with the typical high shear stress values at the spur tip (Koken & Constantinescu, 2008; Rajaratnam & Nwachukwu, 1983) may provide a challenging flow environment for the smolts (Russon, Kemp, & Calles, 2010; Silva, Santos, Ferreira, Pinheiro, & Katopodis, 2011). Changing the spill from the northern to the southern gate simply changed the flow directions downstream of the intake but had no effects on the flow towards the intake. It is thus highly unlikely that this simple measure would decrease the probability of smolts entering the intake. According to the modelling results, the only flow alteration measure with potential for positive effects was the river bank adjustment that reduced velocities and widened the southern flow. Although the strong northern bank flow towards the intake was only marginally reduced and if any, small effects are expected, the generally reduced velocities may allow the smolt to respond more readily to supplementing mitigation measures such as attraction or repulsion devices like fish guidance booms.

Although several of the modelled measures likely would have been regarded as promising solutions, even by hydraulic and fish migration scholars, the hydraulic modelling deemed them at best as of minor use.

The floating booms designed to guide fish rather than the flow also influenced the velocity fields, and particularly, the solid boom combined with changing the gates from the northern to the southern created a distinct flow away from the intake and towards the gate. However, this solution is challenged by strong vertical flow under the boom that the fish is likely to follow (they do so at the intake with a wall extending even deeper), and it is unlikely that such a floating device could actually withstand the drag forces and maintain position and function during flooding conditions, typically appearing during smolt migration.

The rack type permeable boom solution analysed appears as the most promising solution. It was modelled as a 75 m long rack with horizontal bars and angled 30° relative to the bank and the flow direction. Because the surface water (1 m) flow through the rack, only small downwards velocities emerged for the fish to follow. Because the fish cannot pass through the gaps and smolts generally avoid both the structures and the resulting turbulence (Enders et al., 2012; Nestler et al., 2008; Williams et al., 2012), they may migrate along the angled boom to reach the southern flow towards the gates. It has been shown that fish guidance systems such as fish-friendly trash-racks or trash-booms placed upstream of the intake are viable solutions to guide fish away from HPP intakes (Albayrak et al., 2018; Boes et al., 2016; Calles et al., 2013; de Bie, Peirson, & Kemp, 2018; Nestler et al., 2008; Tomanova et al., 2018). In particular, Nyqvist et al. (2017), who analysed migration data from a very similar angled rack with horizontal bars, documented high guiding effectively for salmon towards the bypass channel at a HPP dam and intake facility in Sweden but with a full depth rack.

5 | CONCLUSION

The present study illustrated the value of using river reach CFD modelling as a tool for early evaluation of different mitigation measures to prevent fish entering water intakes to hydropower turbines or other installations and particularly so when combined with high resolution positional telemetry. Further analyses of migration tracks and work towards more detailed and general fish migration models may further improve the value of the approach. Modern measurement instrument (such as ADCP) provide rapid and cost-effective mapping and commercially available software and faster computers now allow efficient CFD modelling at river reach scales. The present modelling was rather extensive (involving the use of high performance computer) because the grid was designed for research purposes, but more coarse grids and modelling on ordinary PCs should be sufficient for more applied purposes. Obviously, the cost of such modelling is far lower than actual construction of measures and assessment of its effects, particularly if the mitigation measures fails and must be revised. We advocate that fish migration challenges at hydroelectric facilities should be explored in advance by a similar approach to provide well-funded engineering solutions for effective fish passage. Although the actual effect of the chosen mitigation measure must be evaluated after implementation, the number and cost of trials are expected to be strongly reduced.

ACKNOWLEDGEMENTS

The presented study was supported by the SafePASS project (no. 244022) funded by the Research Council of Norway (RCN) through the ENERGIX program. The simulations on HPC system were performed on resources provided by UNINETT Sigma 2 the National Infrastructure for High Performance Computing and Data Storage in Norway.

ORCID

Marcell Szabo-Meszaros https://orcid.org/0000-0001-5221-8317

REFERENCES

Akaike, H. (1974). New look at statistical-model identification. *IEEE Transactions on Automatic Control*, *Ac19*(6), 716–723. https://doi.org/10.1109/Tac.1974.1100705

Albayrak, I., Kriewitz, C. R., Hager, W. H., & Boes, R. M. (2018). An experimental investigation on louvres and angled bar racks. *Journal of Hydraulic Research*, *56*(1), 59–75. https://doi.org/10.1080/00221686.2017.1289265

Baktoft, H., Gjelland, K. Ø., Økland, F., & Thygesen, U. H. (2017). Positioning of aquatic animals based on time-of-arrival and random walk models using YAPS (Yet Another Positioning Solver). *Scientific Reports*, *7*(1), 14294. https://doi.org/10.1038/s41598-017-14278-z

Boes, R., Albayrak, I., Kriewitz, C. R., & Peter, A. (2016). Fish protection and downstream fish migration by means of guidance systems with vertical bars: Head loss and bypass efficiency. *WasserWirtschaft*, *106*(7–8), 29–35.

Bunt, C. M., Castro-Santos, T., & Haro, A. (2012). Performance of fish passage structures at upstream barriers to migration. *River Research and Applications*, *28*(4), 457–478. https://doi.org/10.1002/rra.1565

Calles, O., Karlsson, S., Hebrand, M., & Comoglio, C. (2012). Evaluating technical improvements for downstream migrating diadromous fish at a hydroelectric plant. *Ecological Engineering*, *48*, 30–37. https://doi.org/10.1016/j.ecoleng.2011.05.002

Calles, O., Karlsson, S., Vezza, P., Comoglio, C., & Tielman, J. (2013). Success of a low-sloping rack for improving downstream passage of silver eels at a hydroelectric plant. *Freshwater Biology*, *58*(10), 2168–2179. https://doi.org/10.1111/fwb.12199

Calles, O., Olsson, I. C., Comoglio, C., Kemp, P. S., Blunden, L., Schmitz, M., & Greenberg, L. A. (2010). Size-dependent mortality of migratory silver eels at a hydropower plant, and implications for escapement to the sea. *Freshwater Biology*, *55*(10), 2167–2180. https://doi.org/10.1111/j.1365-2427.2010.02459.x

de Bie, J., Peirson, G., & Kemp, P. S. (2018). Effectiveness of horizontally and vertically oriented wedge-wire screens to guide downstream moving juvenile chub (*Squalius cephalus*). *Ecological Engineering*, *123*, 127–134. https://doi.org/10.1016/j.ecoleng.2018.07.038

DWA. (2005). Fish Protection Technologies and Downstream Fishways. Dimensioning, Design, Effectiveness Inspection. Hennef, DWA German Association for Water, Wastewater and Waste.

Enders, E. C., Gessel, M. H., Anderson, J. J., & Williams, J. G. (2012). Effects of decelerating and accelerating flows on juvenile salmonid behavior. *Transactions of the American Fisheries Society*, *141*(2), 357–364. https://doi.org/10.1080/00028487.2012.664604

Electric Power Research Institute (EPRI) and Dominion Millstone Laboratories (DML). (2001). Evaluation of angled bar racks and louvers for guiding fish at water intakes. Report 1005193: 106. Palo Alto, CA and Waterford, CT.

Fjeldstad, H. P., Pulg, U., & Forseth, T. (2018). Safe two-way migration for salmonids and eel past hydropower structures in Europe:A review and recommendations for best-practice solutions. *Marine and Freshwater Research*, *69*(12), 1834–1847. https://doi.org/10.1071/Mf18120

Fjeldstad, H. P., Uglem, I., Diserud, O. H., Fiske, P., Forseth, T., Kvingedal, E., & Jarnegren, J. (2012). A concept for improving Atlantic salmon *Salmo salar* smolt migration past hydro power intakes. *Journal of Fish Biology*, *81*(2), 642–663. https://doi.org/10.1111/j.1095-8649.2012.03363

Fuentes-Perez, J. F., Silva, A. T., Tuhtan, J. A., Garcia-Vega, A., Carbonell-Baeza, R., Musall, M., & Kruusmaa, M. (2018). 3D modelling of non-uniform and turbulent flow in vertical slot fishways. *Environmental Modelling & Software*, *99*, 156–169. https://doi.org/10.1016/j.envsoft.2017.09.011

Gisen, D. C., Weichert, R. B., & Nestler, J. M. (2017). Optimizing attraction flow for upstream fish passage at a hydropower dam employing 3D Detached-Eddy simulation. *Ecological Engineering*, *100*, 344–353. https://doi.org/10.1016/j.ecoleng.2016.10.065

Goodwin, R. A., Nestler, J. M., Anderson, J. J., Weber, L. J., & Loucks, D. P. (2006). Forecasting 3-D fish movement behavior using a Eulerian-Lagrangian-agent method (ELAM). *Ecological Modelling*, *192*(1–2), 197–223. https://doi.org/10.1016/j.ecolmodel.2005.08.004

Greenshields, C. J. (2015). The Open Source CFD toolbox (version 4.1.0). OpenFOAM Foundation ltd.

Havn, T. B., Thorstad, E. B., Teichert, M. A. K., Sæther, S. A., Heermann, L., Hedger, R. D., & Økland, F. (2017). Hydropower-related mortality and behaviour of Atlantic salmon smolts in the River Sieg, a German tributary to the Rhine. *Hydrobiologia*, *805*, 273–290. https://doi.org/10.1007/s10750-017-3311-3

Higuera, P., Lara, J. L., & Losada, I. J. (2013). Realistic wave generation and active wave absorption for Navier-Stokes models Application to OpenFOI(R). *Coastal Engineering*, *71*, 102–118. https://doi.org/10.1016/j.coastaleng.2012.07.002

Jansen, H. M., Winter, H. V., Bruijs, M. C. M., & Polman, H. J. G. (2007). Just go with the flow? Route selection and mortality during downstream migration of silver eels in relation to river discharge. *ICES Journal of Marine Science*, *64*(7), 1437–1443. https://doi.org/10.1093/icesjms/fsm132

Johnston, C. E., & Eales, J. G. (1970). Influence of body size on silvering of Atlantic salmon (*Salmo salar*) at parr-smolt transformation. *Journal of the Fisheries Research Board of Canada*, *27*(5), 983–987. https://doi.org/10.1139/f70-114

Katopodis, C., & Williams, J. G. (2012). The development of fish passage research in a historical context. *Ecological Engineering*, *48*, 8–18. https://doi.org/10.1016/j.ecoleng.2011.07.004

Khan, L. A., Roy, E. W., & Rashid, M. (2008). Computational fluid dynamics modelling of forebay hydrodynamics created by a floating juvenile fish collection facility at the Upper Baker River Dam, Washington. *River Research and Applications*, *24*(9), 1288–1309. https://doi.org/10.1002/rra.1124

Koken, M., & Constantinescu, G. (2008). An investigation of the flow and scour mechanisms around isolated spur dikes in a shallow open channel: 2. Conditions corresponding to the final stages of the erosion and deposition process. *Water Resources Research*, (8). Artn W08407), 44. https://doi.org/10.1029/2007wr006491

Larinier, M. (2008). Fish passage experience at small-scale hydro-electric power plants in France. *Hydrobiologia*, *609*, 97–108. https://doi.org/10.1007/s10750-008-9398-9

Le Coz, J., Blanquart, B., Pobanz, K., Dramais, G., Pierrefeu, G., Hauet, A., & Despax, A. (2016). Estimating the uncertainty of streamgauging techniques using in situ collaborative interlaboratory experiments. *Journal of Hydraulic Engineering*, *142*(7), 04016011. https://doi.org/10.1061/(ASCE)HY.1943-7900.0001109

Li, X. Y., Deng, Z. Q. D., Fu, T., Brown, R. S., Martinez, J. J., McMichael, G. A., & Townsend, R. L. (2018). Three-dimensional migration behavior of juvenile salmonids in reservoirs and near dams. *Scientific Reports*, *8*. ARTN, 956. https://doi.org/10.1038/s41598-018-19208-1

Mardia, K., & Jupp, P. (2010). *Directional statistics*. Chichester: J. Wiley. https://doi.org/10.1002/9780470316979

Metcalfe, J., & Craig, J. F. (2012). Fish migration in [th]e 21st Century: Opportunities and challenges. *Journal of Fish Biology*, *81*(2), 361–364. https://doi.org/10.1111/j.1095-8649.2012.03388.x

Nestler, J. M., Goodwin, R. A., Smith, D. L., Anderson, J. J., & Li, S. (2008). Optimum fish passage and guidance designs are based in the hydrogeomorphology of natural rivers. *River Research and Applications*, *24*(2), 148–168. https://doi.org/10.1002/rra.1056

Nyqvist, D., Nilsson, P. A., Alenäs, I., Elghagen, J., Hebrand, M., Karlsson, S., & Calles, O. (2017). Upstream and downstream passage of migrating adult Atlantic salmon: Remedial measures improve passage performance at a hydropower dam. *Ecological Engineering*, *102*, 331–343. https://doi.org/10.1016/j.ecoleng.2017.02.055

Parsons, D. R., Jackson, P. R., Czuba, J. A., Engel, F. L., Rhoads, B. L., Oberg, K. A., & Riley, J. D. (2013). Velocity Mapping Toolbox (VMT): A processing and visualization suite for moving-vessel ADCP measurements. *Earth Surface Processes and Landforms*, *38*(11), 1244–1260. https://doi.org/10.1002/esp.3367

Pedersen, M. I., Jepsen, N., Aarestrup, K., Koed, A., Pedersen, S., & Okland, F. (2012). Loss of European silver eel passing a hydropower station. *Journal of Applied Ichthyology*, *28*(2), 189–193. https://doi.org/10.1111/j.1439-0426.2011.01913.x

R Development Core Team, 2018. R: A Language and Environment for Statistical Computing. R Foundation for Statistical Computing, Vienna Austria.

Rajaratnam, N., & Nwachukwu, B. A. (1983). Flow near groin-like structures. *Journal of Hydraulic Engineering-Asce*, *109*(3), 463–480. https://doi.org/10.1061/(Asce)0733-9429(1983)109:3(463

Rivinoja, P. (2005). Migration problems of Atlantic salmon (*Salmo salar* L.) in flow regulated rivers. PhD Thesis. Swedish University of Agricultural Science, Department of Aquaculture, Umea, Sweden

Russon, I. J., Kemp, P. S., & Calles, O. (2010). Response of downstream migrating adult European eels (*Anguilla anguilla*) to bar racks under experimental conditions. *Ecology of Freshwater Fish*, *19*(2), 197–205. https://doi.org/10.1111/j.1600-0633.2009.00404.x

Scruton, D. A., McKinley, R. S., Kouwen, N., Eddy, W., & Booth, R. K. (2003). Improvement and optimization of fish guidance efficiency (FGE) at a behavioural fish protection system for downstream migrating atlantic salmon (Salmo salar) smolts. *River Research and Applications*, *19*(5–6), 605–617. https://doi.org/10.1002/rra.735

Scruton, D. A., Pennell, C. J., Bourgeois, C. E., Goosney, R. F., Porter, T. R., & Clarke, K. D. (2007). Assessment of a retrofitted downstream fish bypass system for wild Atlantic salmon (*Salmo salar*) smolts and kelts at a hydroelectric facility on the Exploits River, Newfoundland, Canada. *Hydrobiologia*, *582*, 155–169. https://doi.org/10.1007/s10750-006-0557-6

Silva, A. T., Lucas, M. C., Castro-Santos, T., Katopodis, C., Baumgartner, L. J., Thiem, J. D., … Cooke, S. J. (2018). The future of fish passage science, engineering, and practice. *Fish and Fisheries*, *19*(2), 340–362. https://doi.org/10.1111/faf.12258

Silva, A. T., Santos, J. M., Ferreira, M. T., Pinheiro, A. N., & Katopodis, C. (2011). Effects of water velocity and turbulence on the behaviour of Iberian barbel (*Luciobarbus Bocagei*, Steindachner 1864) in an experimental pool-type fishway. *River Research and Applications*, *27*(3), 360–373. https://doi.org/10.1002/rra.1363

Szabo-Meszaros, M., Navaratnam, C. U., Aberle, J., Silva, A. T., Forseth, T., Calles, O., … Alfredsen, K. (2018). Experimental hydraulics on fish-friendly trash-racks: An ecological approach. *Ecological Engineering*, *113*, 11–20. https://doi.org/10.1016/j.ecoleng.2017.12.032

Thorstad, E. B., Havn, T. B., Sæther, S. A., Heermann, L., Teichert, M. A. K., Diserud, O. H., … Økland, F. (2017). Survival and behaviour of Atlanic salmon smolts passing a run- of- river hydropower facility with a movable bulb turbine. *Fisheries Management and Ecology*, *24*(3), 199–207. https://doi.org/10.1111/fme.12216

Thorstad, E. B., Whoriskey, F., Rikardsen, A. H., & Aarestrup, K. (2011). Aquatic nomads: The life and migrations of the Atlantic salmon. In Ø. Aas, S. Einum, A. Klemetsen, & J. Skurdal (Eds.), *Atlantic salmon ecology* (1st ed.). Wiley-Blackwell.

Tomanova, S., Courret, D., Alric, A., De Oliveira, E., Lagarrigue, T., & Tétard, S. (2018). Protecting efficiently sea-migrating salmon smolts from entering hydropower plant turbines with inclined or oriented low bar spacing racks. *Ecological Engineering*, *122*, 143–152. https://doi.org/10.1016/j.ecoleng.2018.07.034

Wilkes, M., Baumgartner, L., Boys, C., Silva, L. G. M., O'Connor, J., Jones, M., & Webb, J. A. (2018). Fish-Net: Probabilistic models for fishway planning, design and monitoring to support environmentally sustainable hydropower. *Fish and Fisheries*, *19*(4), 677–697. https://doi.org/10.1111/faf.12282

Williams, J. G., Armstrong, G., Katopodis, C., Lariniere, M., & Travade, F. (2012). Thinking like a fish: A key ingredient for development of effective fish passage facilities at river obstructions. *River Research and Applications*, *28*(4), 407–417. https://doi.org/10.1002/rra.1551

Zuur, A. F., Hilbe, J. M. & Ieno, E. N. (2013) A Beginner's Guide to GLM and GLMM with R. a frequentist and Bayesian perspective for ecologists. Newburgh, United Kingdom: Highland Statistics Ltd.

How to cite this article: Szabo-Meszaros M, Forseth T, Baktoft H, et al. Modelling mitigation measures for smolt migration at dammed river sections. *Ecohydrology*. 2019; 12:e2131. https://doi.org/10.1002/eco.2131